

Dynamic Downlink-Uplink Spectrum Sharing between Terrestrial and Non-Terrestrial Networks

Sourav Mukherjee*, Bho Matthiesen*, Armin Dekorsy*, Petar Popovski^{†*}

*University of Bremen, Department of Communications Engineering, Germany

[†]Aalborg University, Department of Electronic Systems, Denmark

email: {mukherjee, matthiesen, dekorsy}@ant.uni-bremen.de, petarp@es.aau.dk

Abstract—6G networks are expected to integrate low Earth orbit satellites to ensure global connectivity by extending coverage to underserved and remote regions. However, the deployment of dense mega-constellations introduces severe interference among satellites operating over shared frequency bands. This is, in part, due to the limited flexibility of conventional frequency division duplex (FDD) systems, where fixed bands for downlink (DL) and uplink (UL) transmissions are employed. In this work, we propose dynamic re-assignment of FDD bands for improved interference management in dense deployments and evaluate the performance gain of this approach. To this end, we formulate a joint optimization problem that incorporates dynamic band assignment, user scheduling, and power allocation in both directions. This non-convex mixed integer problem is solved using a combination of equivalence transforms, alternating optimization, and state-of-the-art industrial-grade mixed integer solvers. Numerical results demonstrate that the proposed approach of dynamic FDD band assignment significantly enhances system performance over conventional FDD, achieving up to 94 % improvement in throughput in dense deployments.

Index Terms—Spectrum sharing, Dynamic downlink-uplink band, LEO, interference-mitigation.

I. INTRODUCTION

The non-terrestrial network (NTN) is pivotal for realizing the long-standing vision of global coverage and bridging the digital divide [1]. Among the others, low Earth orbit (LEO) constellations are envisioned as a cornerstone of future technologies, thanks to their lower launching cost, lower path-loss, and delay. Further, due to ambitious projects by Iridium, OneWeb, SpaceX, Amazon, and Europe’s IRIS², the LEO will likely become crowded. Forcing multiple satellites in different orbits to share the frequency bands.

To enable spectrum sharing, the early works focus in between the geostationary Earth orbit (GEO) and non-geostationary Earth orbit satellites, comparing traditional methods like look-aside [2] among others. However, these methods suffer from high aggregated interference at the receiver [3]. A significant amount of literature also explores spectrum sharing between terrestrial and satellite. Notably, a key technique which uses reverse pairing were proposed for flexible utilization of frequency bands to reduce the interference [4]. In normal pairing, both systems use the same band

This work is supported by the German Research Foundation (DFG) under Grant EXC 2077 (University Allowance).

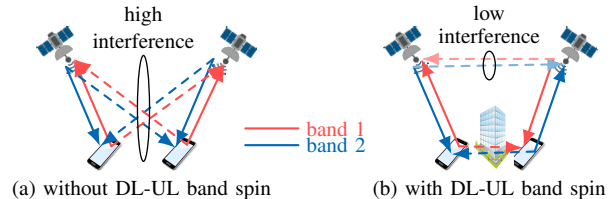


Fig. 1. Motivation for dynamic downlink-uplink (DL-UL) band selection, shown for two satellites: (a) Fixed-band allocation, each satellite uses predetermined DL and UL bands, leading to strong interference. (b) Dynamic band selection, satellites flexibly assign bands for DL or UL, reducing inter-satellite interference through spatial separation and directive antennas.

for downlink (DL) and another shared band for uplink (UL). By contrast, reverse pairing assigns one band to the DL of one system and the UL of the other, and vice-versa for the second band. More recent studies shifted attention towards LEO-LEO, by providing various methods to reduce interference [5], [6]. However, the existing interference mitigation techniques provide limited gain in high-interference scenarios; therefore, an effective strategy is desired, due to emerging dense LEO constellations.

In this work, we propose a novel scheduling methodology for satellites operating on common bands, where the two fixed frequency bands can dynamically switch roles between DL and UL. This flexibility introduces an additional degree-of-freedom in scheduling, and improve the overall system performance. The selection of DL and UL frequency bands from the two available options is treated as a variable, which we refer to as the *spin*, and the overall mechanism is termed *spinning bands*. The idea of spin is inspired by [7], where authors optimized the transmission directions of DL and UL in a time-division duplex system.

To appreciate the advantages of dynamic DL-UL band selection in the satellite systems, consider an example illustrated in Fig. 1. In a conventional setup, Fig. 1(a), each satellite communicates with its own user-equipment (UE) using fixed frequency bands for DL and UL. When these bands are reused across satellites, interference arises. Now consider the alternative in Fig. 1(b), where the satellites are granted the flexibility to dynamically assign the direction of transmission for each band, and assume the satellites use different bands for DL, correspondingly for UL. In this case, the dominant

source of interference shifts to satellite-to-satellite and UE-to-UE links. Since, the satellites are generally separated by a large distances and equipped with highly directive antennas, this reduces the satellite-satellite interference. Therefore, the only source of interference is UE-UE. As the UE-UE channel depending on the environment maybe heavily attenuated, and also modern UEs are equipped with multiple patch antennas and capable of UL beamforming, thereby choosing opposite bands may become an essential tool for increasing the throughput. However, for more than two satellites, the decision becomes more challenging and even with high UE-UE interference, depending on the UE distributions, assigning different DL and UL bands to different systems may lead to increase in throughput. This motivates us to formulate a joint optimization problem that incorporates dynamic band assignment, user scheduling, and power allocation.

The rest of the paper is organized as follows: the system model, then the optimization problem involving spin, power, and scheduling is presented in Section II. The solution approach to the optimization is discussed in Section III, numerical results are presented in Section IV, and finally conclusions are drawn in Section V.

II. SYSTEM MODEL & PROBLEM FORMULATION

Consider a group comprising J LEO satellites, each equipped with N antennas, serving a region with a total of K single-antenna UEs, as illustrated in Fig. 2. In this work, the problem formulation is done over a single snapshot, during which the satellite positions and resource allocations are assumed to remain fixed. The satellites and UEs are indexed by the sets $\mathcal{J} = \{1, \dots, J\}$ and $\mathcal{K} = \{1, \dots, K\}$, respectively. Two frequency bands are available for DL and UL communications, where band l , $l \in \{1, 2\}$, has center frequency f_l and bandwidth B_l . Satellite $j \in \mathcal{J}$ serves a subset of the UEs on these bands. Each UE maintains separate connections for DL and UL, either to the same or to separate satellites. UE association to satellite j in the DL is indicated by a binary variable $d_{kj} \in \{0, 1\}$, where $d_{kj} = 1$ means UE k is served in DL by satellite j , and $d_{kj} = 0$ otherwise. Similarly, UL association is indicated by a binary variable $u_{kj} \in \{0, 1\}$, where $u_{kj} = 1$ means UE k is served in UL by the satellite j , and $u_{kj} = 0$ otherwise. The band assignment for satellite j is represented by spin binary variable $r_j \in \{0, 1\}$. If $r_j = 1$, band $l = 1$ is used for DL and band $l = 2$ for UL; if $r_j = 0$, the roles of the bands are reversed, as illustrated in Fig. 3. This is, essentially, a frequency-division duplex system at the satellite j with improved interference management capabilities through flexible band assignment. Still, each transceiver has to use orthogonal frequency bands for UL and DL transmissions. At UE k , this can be enforced by the condition $\sum_{j \in \mathcal{J}} d_{kj} r_j = \sum_{j \in \mathcal{J}} u_{kj} r_j$. This, however, is only necessary if the UE is simultaneously served in DL

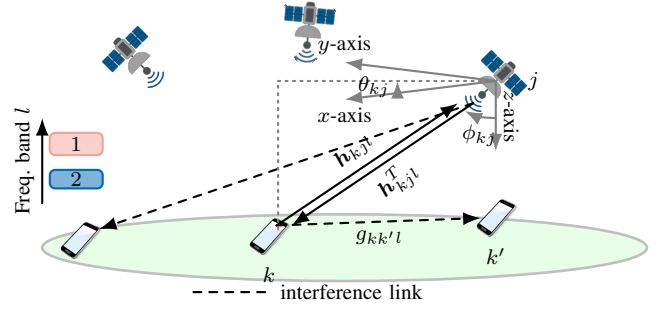


Fig. 2. A system of J LEO satellites in orbit serving K UEs over region.

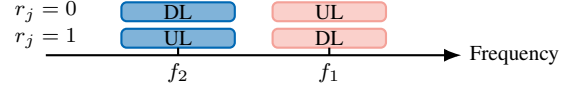


Fig. 3. Introduced spin variable for a satellite j .

and UL. Thus,

$$\sum_{j \in \mathcal{J}} d_{kj} = 1 \quad \text{and} \quad \sum_{j \in \mathcal{J}} u_{kj} = 1$$

$$\implies \sum_{j \in \mathcal{J}} d_{kj} r_j = \sum_{j \in \mathcal{J}} u_{kj} r_j. \quad (1)$$

For all other cases, this condition is not relevant.

We denote the band- l channel from satellite j to UE k as $\mathbf{h}_{kjl} \in \mathbb{C}^{N \times 1}$. This channel has a dominant line-of-sight (LOS) component with only small non-LOS effects in the ground-segment. The UEs are assumed to know their own position and those of all satellites. In particular, let m_{kj} , θ_{kj} , and ϕ_{kj} be the distance, azimuth, and elevation angle from satellite j to UE k . Then, the LOS component of \mathbf{h}_{kjl} is $\sqrt{\beta_{kjl}} \mathbf{b}_l(\theta_{kj}, \phi_{kj})$ with path loss $\beta_{kjl} = (c/4\pi m_{kj} f_l)^2$ and array-response vector as

$$\mathbf{b}_l = \left(\left[\exp \left(-\frac{j2\pi f_l}{c} (D_n^x \psi^x + D_n^y \psi^y) \right) \right]_{n=1}^N \right)^T, \quad (2)$$

where $\psi^x = \cos(\phi_{kj}) \cos(\theta_{kj})$, $\psi^y = \cos(\phi_{kj}) \sin(\theta_{kj})$, and D_n^x, D_n^y denote the x and y -coordinate, respectively of n -th antenna element. We model \mathbf{h}_{kjl} as purely LOS but note that statistical channel state information (CSI) is straightforward to incorporate into β_{kjl} . Further, we assume negligible interference between satellites due to the high directivity and downward positioning of satellite antenna array. However, we need to take inter-UE interference into account. Since accurate and instantaneous inter-UE CSI is infeasible to obtain, we model the band- l channel $g_{kk'l} = g_{k'kl}$ from UE k to k' based on position-dependent long-term statistics.

Now, consider that UE k is served by satellite j in the DL, indicated by the binary variable $d_{kj} = 1$. The effective DL interference channel from satellite $j' \in \mathcal{J}$ to k , while serving another UE $k' \in \mathcal{K}_{-k}$ in the DL (i.e., $d_{k'j'} = 1$), is given by

$$(\gamma_{kjj'}^{\text{dl}})^T = \overline{|r_j - r_{j'}|} [r_{j'} \mathbf{h}_{k'j',l=1}^T + \overline{r_{j'}} \mathbf{h}_{k'j',l=2}^T], \quad (3)$$

where r_j and $r_{j'}$ denote the spins of satellites j and j' , and $|r_j - r_{j'}|$ captures the relative spin between them. This interference arises when both satellites operate with the same spin. Here, \bar{a} denotes the binary complement of $a \in \{0, 1\}$, and for a set \mathcal{A} , $\mathcal{A}_{-i} = \mathcal{A} \setminus \{i\}$ for $i \in \mathcal{A}$. Note that $\gamma_{kjj'}^{\text{dl}}$ also represents the direct DL channel between satellite j and UE k when $j' = j$, since $|r_j - r_j| = 1$. Similarly, if UE k is served by satellite j in the UL, indicated by $u_{kj} = 1$, then the effective UL interference channel from UE $k' \in \mathcal{K}$ to satellite j , where k' is served by satellite $j' \in \mathcal{J}$ in the UL (i.e., $u_{k'j'} = 1$), is

$$\gamma_{k'jj'}^{\text{ul}} = |r_j - r_{j'}| [r_{j'} \mathbf{h}_{k'j,l=2} + \bar{r}_{j'} \mathbf{h}_{k'j,l=1}]. \quad (4)$$

Note that, $\gamma_{k'jj'}^{\text{ul}}$ also captures the direct UL channel from UE k to satellite j when $k' = k$ and $j' = j$; and this interference arises when both satellites operate with the same spin. Additionally, a UE may cause interference to another UE during UL transmission. Suppose UE $k' \in \mathcal{K}_{-k}$ is served in the UL by satellite $j' \in \mathcal{J}_{-j}$ (i.e., $u_{k'j'} = 1$), while UE k is served in the DL by satellite j (i.e., $d_{kj} = 1$). Then, the effective interference channel from UE k' to UE k is given by

$$\nu_{kk'jj'} = |r_j - r_{j'}| [r_{j'} g_{k'l=1} + \bar{r}_{j'} g_{k'l=2}], \quad (5)$$

where $\nu_{kk'jj'} = \nu_{k'kj'j'}$ due to reciprocity. This interference only arises if the spins of the associated satellites j and j' are opposite.

The received signals at UE k in the DL and at satellite j in the UL, corresponding to link kj , are denoted by y_{kj}^{dl} and y_{kj}^{ul} , respectively, and can be expressed as

$$\begin{aligned} y_{kj}^{\text{dl}} &= d_{kj} \sqrt{p_k^{\text{dl}}} \|\gamma_{kjj}^{\text{dl}}\| s_k^{\text{dl}} \\ &+ \sum_{j' \in \mathcal{J}} \sum_{k' \in \mathcal{K}_{-k}} d_{k'j'} \sqrt{p_{k'}^{\text{dl}}} (\gamma_{kjj'}^{\text{dl}})^T \mathbf{w}_{k'j'} s_{k'}^{\text{dl}} \\ &+ \sum_{j' \in \mathcal{J}_{-j}} \sum_{k' \in \mathcal{K}_{-k}} u_{k'j'} \sqrt{p_{k'}^{\text{ul}}} \nu_{kk'jj'} s_{k'}^{\text{ul}} + n_{kj}^{\text{dl}}, \end{aligned} \quad (6a)$$

$$\begin{aligned} y_{kj}^{\text{ul}} &= u_{kj} \sqrt{p_k^{\text{ul}}} \|\gamma_{kjj}^{\text{ul}}\| s_k^{\text{ul}} \\ &+ \sum_{j' \in \mathcal{J}} \sum_{k' \in \mathcal{K}_{-k}} u_{k'j'} \sqrt{p_{k'}^{\text{ul}}} \mathbf{v}_{k'j'}^T \gamma_{k'jj'}^{\text{ul}} s_{k'}^{\text{ul}} + n_{kj}^{\text{ul}}, \end{aligned} \quad (6b)$$

where $\mathbf{w}_{k'j'} \in \mathbb{C}^{N \times 1}$ denotes the DL maximal-ratio transmission (MRT) precoder for link $k'j'$, and the vector $\mathbf{v}_{kj} \in \mathbb{C}^{N \times 1}$ is the maximal-ratio combiner (MRC) receiver at satellite j for UE k in the UL. Additionally, s_k^{dl} denotes the unit-energy symbol transmitted in the DL towards UE k' , whereas $s_{k'}^{\text{ul}}$ represents the unit-energy symbol transmitted by UE k' in the UL. The receiver noise terms n_{kj}^{dl} for the DL and n_{kj}^{ul} for the UL are modeled as complex Gaussian with mean 0 and variance σ^2 . The corresponding transmit powers are denoted by $p_{k'}^{\text{dl}}$ for the DL, i.e., from satellite to UE k' , and by $p_{k'}^{\text{ul}}$ for the UL, i.e., from UE k' to the satellite.

A. Formulation of the Optimization Problem

We formulate a joint optimization problem considering user association, power control, and spins. The objective is the sum

of both DL and UL spectral efficiency for all possible user-satellite pairs, and the mathematical program is written as

$$\begin{aligned} (\text{P0}) : \quad & \max_{\mathbf{d}, \mathbf{r}, \mathbf{u}, \mathbf{p}^{\text{dl}}, \mathbf{p}^{\text{ul}}} f_0(\mathbf{d}, \mathbf{r}, \mathbf{u}, \mathbf{p}^{\text{dl}}, \mathbf{p}^{\text{ul}}) \\ \text{s.t.} \quad & \text{FDD condition in (1), for all } k \end{aligned} \quad (8a)$$

$$\sum_{j \in \mathcal{J}} d_{kj} \leq 1, \sum_{j \in \mathcal{J}} u_{kj} \leq 1, \text{ for all } k \quad (8b)$$

$$\sum_{k \in \mathcal{K}} d_{kj} p_k^{\text{dl}} \leq p_j^{\text{max}}, \text{ for all } j \quad (8c)$$

$$p_k^{\text{ul}} \leq p_k^{\text{max}}, \text{ for all } k \quad (8d)$$

$$p_k^{\text{dl}} \geq 0, p_k^{\text{ul}} \geq 0, \text{ for all } k \quad (8e)$$

$$d_{kj}, r_j, u_{kj} \in \{0, 1\}, \text{ for all } k \text{ and } j. \quad (8f)$$

Here, $\mathbf{d} = [d_{kj}]_{k=1, j=1}^{k=K, j=J}$, $\mathbf{u} = [u_{kj}]_{k=1, j=1}^{k=K, j=J}$, $\mathbf{r} = [r_j]_{j=1}^J$, $\mathbf{p}^{\text{dl}} = [p_k^{\text{dl}}]_{k=1}^K$, and $\mathbf{p}^{\text{ul}} = [p_k^{\text{ul}}]_{k=1}^K$. The objective f_0 is defined in (7). Constraint (8b) restricts each UE to connect with at most one satellite in DL and at most one in UL. Constraint (8c) limits the total DL transmit power of each satellite j to its maximum budget p_j^{max} , while (8d) ensures that each UE k does not exceed its own UL transmit power budget p_k^{max} . Constraint (8e) enforces non-negativity of all power variables, and (8f) implies that the scheduling and spin variables are binary.

III. SOLUTION TO (P0)

The mathematical program in (8) is non-convex due to sum of logarithmic functions of signal-to-noise plus interference ratios (SINRs), and the SINR is expressed as ratio of sums containing product of continuous power and binary variables. To solve, we do an equivalent transform, first using Lagrangian dual transform [8], to take out the SINR outside logarithm; then, we apply Quadratic transform [8], to make the ratios into a sum of two terms. After transformation, we do alternating optimization to solve the transformed problem, where we update block of variables. Finally, the algorithm is described.

First, we apply Lagrangian dual transform from Theorem 3 in [8] to transform the problem in (P0) as

$$\begin{aligned} (\text{P1}) : \quad & \max_{\mathbf{d}, \mathbf{r}, \mathbf{u}, \mathbf{p}^{\text{dl}}, \mathbf{p}^{\text{ul}}, \boldsymbol{\chi}^{\text{dl}}, \boldsymbol{\chi}^{\text{ul}}} f_1(\mathbf{d}, \mathbf{r}, \mathbf{u}, \mathbf{p}^{\text{dl}}, \mathbf{p}^{\text{ul}}, \boldsymbol{\chi}^{\text{dl}}, \boldsymbol{\chi}^{\text{ul}}) \\ \text{s.t.} \quad & (8a) - (8f), \quad \chi_{kj}^{\text{dl}}, \chi_{kj}^{\text{ul}} \in \mathbb{R}_+ \end{aligned} \quad (11a)$$

where with the auxiliary variables $\boldsymbol{\chi}^{\text{dl}} = [\chi_{kj}^{\text{dl}}]_{k=1, j=1}^{k=K, j=J}$ and $\boldsymbol{\chi}^{\text{ul}} = [\chi_{kj}^{\text{ul}}]_{k=1, j=1}^{k=K, j=J}$, the objective f_1 is shown at the bottom in (9). Then, we apply the Quadratic transform from Theorem 1 in [8] to transform (P1) as

$$\begin{aligned} (\text{P2}) : \quad & \max_{\mathbf{d}, \mathbf{r}, \mathbf{u}, \mathbf{p}^{\text{dl}}, \mathbf{p}^{\text{ul}}, \boldsymbol{\chi}^{\text{dl}}, \boldsymbol{\chi}^{\text{ul}}, \boldsymbol{\xi}^{\text{dl}}, \boldsymbol{\xi}^{\text{ul}}} f_2(\mathbf{d}, \mathbf{r}, \mathbf{u}, \mathbf{p}^{\text{dl}}, \mathbf{p}^{\text{ul}}, \boldsymbol{\chi}^{\text{dl}}, \boldsymbol{\chi}^{\text{ul}}, \boldsymbol{\xi}^{\text{dl}}, \boldsymbol{\xi}^{\text{ul}}) \\ \text{s.t.} \quad & (8a) - (8f), \end{aligned} \quad (12a)$$

$$\chi_{kj}^{\text{dl}}, \chi_{kj}^{\text{ul}} \in \mathbb{R}_+, \xi_{kj}^{\text{dl}}, \xi_{kj}^{\text{ul}} \in \mathbb{R} \quad (12b)$$

where with the auxiliary variables $\boldsymbol{\xi}^{\text{dl}} = [\xi_{kj}^{\text{dl}}]_{k=1, j=1}^{k=K, j=J}$ and $\boldsymbol{\xi}^{\text{ul}} = [\xi_{kj}^{\text{ul}}]_{k=1, j=1}^{k=K, j=J}$, the objective f_2 is shown at the bottom

in (10). The equivalence between the transformed problems is established below:

Proposition 1. Consider a solution to (P2) given by $(\mathbf{d}^\dagger, \mathbf{r}^\dagger, \mathbf{u}^\dagger, \mathbf{p}^{\text{dl}\dagger}, \mathbf{p}^{\text{ul}\dagger}, \chi^{\text{dl}\dagger}, \chi^{\text{ul}\dagger}, \xi^{\text{dl}\dagger}, \xi^{\text{ul}\dagger})$. Then, the tuple $(\mathbf{d}^\dagger, \mathbf{r}^\dagger, \mathbf{u}^\dagger, \mathbf{p}^{\text{dl}\dagger}, \mathbf{p}^{\text{ul}\dagger}, \chi^{\text{dl}\dagger}, \chi^{\text{ul}\dagger})$ is also a solution to (P1), and further, $(\mathbf{d}^\dagger, \mathbf{r}^\dagger, \mathbf{u}^\dagger, \mathbf{p}^{\text{dl}\dagger}, \mathbf{p}^{\text{ul}\dagger})$ is also a solution to (P0).

Proof. See Appendix A. \square

To solve (P0), we first solve (P2). To solve (P2), we update variables in three blocks: (i) update ξ^{dl} and ξ^{ul} , (ii) update χ^{dl} and χ^{ul} , and (iii) jointly update \mathbf{d} , \mathbf{u} , \mathbf{p}^{dl} , and \mathbf{p}^{ul} . Since the spin variables \mathbf{r} add extra complexity, we perform an exhaustive search over all possible spin configurations.

A. Update χ^{dl} and χ^{ul}

The objective f_1 is strictly concave in χ_{kj}^{dl} and χ_{kj}^{ul} . Hence, by keeping other parameters fixed, the unique optimal value of χ_{kj}^{dl} and χ_{kj}^{ul} can be obtained from $\partial f_1 / \partial \chi_{kj}^{\text{dl}} = 0$ and $\partial f_1 / \partial \chi_{kj}^{\text{ul}} = 0$, respectively, as

$$\begin{aligned} \chi_{kj}^{\text{dl}\star} &= d_{kj} p_k^{\text{dl}} \|\gamma_{kjj}^{\text{dl}}\|^2 \\ &\quad / \left(\sigma^2 + \sum_{j' \in \mathcal{J}} \sum_{k' \in \mathcal{K}_{-k}} d_{k'j'} p_{k'}^{\text{dl}} |(\gamma_{k'jj'}^{\text{dl}})^T \mathbf{w}_{k'j'}|^2 \right. \\ &\quad \left. + \sum_{j' \in \mathcal{J}_{-j}} \sum_{k' \in \mathcal{K}_{-k}} u_{k'j'} p_{k'}^{\text{ul}} |\nu_{kk'jj'}|^2 \right), \end{aligned} \quad (13a)$$

$$\begin{aligned} \chi_{kj}^{\text{ul}\star} &= u_{kj} p_k^{\text{ul}} \|\gamma_{kjj}^{\text{ul}}\|^2 \\ &\quad / \left(\sigma^2 + \sum_{j' \in \mathcal{J}} \sum_{k' \in \mathcal{K}_{-k}} u_{k'j'} p_{k'}^{\text{ul}} |\mathbf{v}_{kj}^T \gamma_{k'jj'}^{\text{ul}}|^2 \right). \end{aligned} \quad (13b)$$

Here, χ_{kj}^{dl} and χ_{kj}^{ul} are updated simultaneously using the above equations, since they are independent of each other.

B. Update ξ^{dl} and ξ^{ul}

The objective f_2 is strictly concave in ξ_{kj}^{dl} and ξ_{kj}^{ul} . Hence, by keeping other parameters fixed, the unique optimal value of ξ_{kj}^{dl} and ξ_{kj}^{ul} can be obtained from $\partial f_2 / \partial \xi_{kj}^{\text{dl}} = 0$ and $\partial f_2 / \partial \xi_{kj}^{\text{ul}} = 0$, respectively, as

$$\begin{aligned} \xi_{kj}^{\text{dl}\star} &= d_{kj} \sqrt{(1 + \chi_{kj}^{\text{dl}}) p_k^{\text{dl}} \|\gamma_{kjj}^{\text{dl}}\|} \\ &\quad / \left(\sigma^2 + \sum_{j' \in \mathcal{J}} \sum_{k' \in \mathcal{K}} d_{k'j'} p_{k'}^{\text{dl}} |(\gamma_{k'jj'}^{\text{dl}})^T \mathbf{w}_{k'j'}|^2 \right. \\ &\quad \left. + \sum_{j' \in \mathcal{J}_{-j}} \sum_{k' \in \mathcal{K}_{-k}} u_{k'j'} p_{k'}^{\text{ul}} |\nu_{kk'jj'}|^2 \right), \end{aligned} \quad (14a)$$

$$\begin{aligned} \xi_{kj}^{\text{ul}\star} &= u_{kj} \sqrt{(1 + \chi_{kj}^{\text{ul}}) p_k^{\text{ul}} \|\gamma_{kjj}^{\text{ul}}\|} \\ &\quad / \left(\sigma^2 + \sum_{j' \in \mathcal{J}} \sum_{k' \in \mathcal{K}} u_{k'j'} p_{k'}^{\text{ul}} |\mathbf{v}_{kj}^T \gamma_{k'jj'}^{\text{ul}}|^2 \right). \end{aligned} \quad (14b)$$

Similar to III-A, ξ_{kj}^{dl} and ξ_{kj}^{ul} are updated simultaneously.

C. Update Jointly \mathbf{d} , \mathbf{u} , \mathbf{p}^{dl} , \mathbf{p}^{ul}

We jointly update $(\mathbf{d}, \mathbf{u}, \mathbf{p}^{\text{dl}}, \mathbf{p}^{\text{ul}})$ as

$$\begin{aligned} (\text{P3}) : \quad &\max_{\mathbf{d}, \mathbf{u}, \mathbf{p}^{\text{dl}}, \mathbf{p}^{\text{ul}}} f_2(\mathbf{d}, \mathbf{r}, \mathbf{u}, \mathbf{p}^{\text{dl}}, \mathbf{p}^{\text{ul}}, \chi^{\text{dl}\star}, \chi^{\text{ul}\star}, \xi^{\text{dl}\star}, \xi^{\text{ul}\star}) \\ &\text{s.t. (8a) - (8f)}. \end{aligned} \quad (15a)$$

The above mathematical program involves the product of the square root of the power variable and a binary variable, as well as the product of the power variable and a binary variable. To handle these nonlinear terms, we apply the following substitutions $t_k^{\text{dl}} = \sqrt{p_k^{\text{dl}}}$, $t_k^{\text{ul}} = \sqrt{p_k^{\text{ul}}}$, for $k = 1, \dots, K$, and define $\mathbf{t}^{\text{dl}} = [t_k^{\text{dl}}]_{k=1}^K$, $\mathbf{t}^{\text{ul}} = [t_k^{\text{ul}}]_{k=1}^K$. This substitution is one-to-one for $t_k^{\text{dl}} \geq 0$ and $t_k^{\text{ul}} \geq 0$. Therefore, both the problems

$$\begin{aligned} f_0(\mathbf{d}, \mathbf{r}, \mathbf{u}, \mathbf{p}^{\text{dl}}, \mathbf{p}^{\text{ul}}) &= \sum_{k \in \mathcal{K}} \sum_{j \in \mathcal{J}} \left[\log_2(1 + u_{kj} p_k^{\text{ul}} \|\gamma_{kjj}^{\text{ul}}\|^2 / (\sigma^2 + \sum_{j' \in \mathcal{J}} \sum_{k' \in \mathcal{K}_{-k}} u_{k'j'} p_{k'}^{\text{ul}} |\mathbf{v}_{kj}^T \gamma_{k'jj'}^{\text{ul}}|^2)) \right. \\ &\quad \left. + \log_2(1 + d_{kj} p_k^{\text{dl}} \|\gamma_{kjj}^{\text{dl}}\|^2 / (\sigma^2 + \sum_{j' \in \mathcal{J}} \sum_{k' \in \mathcal{K}_{-k}} d_{k'j'} p_{k'}^{\text{dl}} |(\gamma_{k'jj'}^{\text{dl}})^T \mathbf{w}_{k'j'}|^2 + \sum_{j' \in \mathcal{J}_{-j}} \sum_{k' \in \mathcal{K}_{-k}} u_{k'j'} p_{k'}^{\text{ul}} |\nu_{kk'jj'}|^2)) \right]. \end{aligned} \quad (7)$$

$$f_1(\mathbf{d}, \mathbf{r}, \mathbf{u}, \mathbf{p}^{\text{dl}}, \mathbf{p}^{\text{ul}}, \chi^{\text{dl}}, \chi^{\text{ul}}) =$$

$$\begin{aligned} &\sum_{k \in \mathcal{K}} \sum_{j \in \mathcal{J}} \left[\log_2(1 + \chi_{kj}^{\text{dl}}) + \log_2(1 + \chi_{kj}^{\text{ul}}) - \chi_{kj}^{\text{dl}} - \chi_{kj}^{\text{ul}} + (1 + \chi_{kj}^{\text{ul}}) u_{kj} p_k^{\text{ul}} \|\gamma_{kjj}^{\text{ul}}\|^2 / (\sigma^2 + \sum_{j' \in \mathcal{J}} \sum_{k' \in \mathcal{K}} u_{k'j'} p_{k'}^{\text{ul}} |\mathbf{v}_{kj}^T \gamma_{k'jj'}^{\text{ul}}|^2) \right. \\ &\quad \left. + (1 + \chi_{kj}^{\text{dl}}) d_{kj} p_k^{\text{dl}} \|\gamma_{kjj}^{\text{dl}}\|^2 / (\sigma^2 + \sum_{j' \in \mathcal{J}} \sum_{k' \in \mathcal{K}} d_{k'j'} p_{k'}^{\text{dl}} |(\gamma_{k'jj'}^{\text{dl}})^T \mathbf{w}_{k'j'}|^2 + \sum_{j' \in \mathcal{J}_{-j}} \sum_{k' \in \mathcal{K}_{-k}} u_{k'j'} p_{k'}^{\text{ul}} |\nu_{kk'jj'}|^2) \right]. \end{aligned} \quad (9)$$

$$\begin{aligned} f_2(\mathbf{d}, \mathbf{r}, \mathbf{u}, \mathbf{p}^{\text{dl}}, \mathbf{p}^{\text{ul}}, \chi^{\text{dl}}, \chi^{\text{ul}}, \xi^{\text{dl}}, \xi^{\text{ul}}) &= \sum_{k \in \mathcal{K}} \sum_{j \in \mathcal{J}} \left[\log_2(1 + \chi_{kj}^{\text{dl}}) + \log_2(1 + \chi_{kj}^{\text{ul}}) - \chi_{kj}^{\text{dl}} - \chi_{kj}^{\text{ul}} + 2\xi_{kj}^{\text{dl}} d_{kj} \sqrt{(1 + \chi_{kj}^{\text{dl}}) p_k^{\text{dl}} \|\gamma_{kjj}^{\text{dl}}\|} \right. \\ &\quad \left. + 2\xi_{kj}^{\text{ul}} u_{kj} \sqrt{(1 + \chi_{kj}^{\text{ul}}) p_k^{\text{ul}} \|\gamma_{kjj}^{\text{ul}}\|} - (\xi_{kj}^{\text{dl}})^2 (\sigma^2 + \sum_{j' \in \mathcal{J}} \sum_{k' \in \mathcal{K}} d_{k'j'} p_{k'}^{\text{dl}} |(\gamma_{k'jj'}^{\text{dl}})^T \mathbf{w}_{k'j'}|^2 + \sum_{j' \in \mathcal{J}_{-j}} \sum_{k' \in \mathcal{K}_{-k}} u_{k'j'} p_{k'}^{\text{ul}} |\nu_{kk'jj'}|^2) \right. \\ &\quad \left. - (\xi_{kj}^{\text{ul}})^2 (\sigma^2 + \sum_{j' \in \mathcal{J}} \sum_{k' \in \mathcal{K}} u_{k'j'} p_{k'}^{\text{ul}} |\mathbf{v}_{kj}^T \gamma_{k'jj'}^{\text{ul}}|^2) \right]. \end{aligned} \quad (10)$$

are equivalent. Then, the continuous-binary product, can be handled by the following substitution

$$z_{kj}^{\text{dl}} = d_{kj}t_k^{\text{dl}}, z_{kj}^{\text{ul}} = u_{kj}t_k^{\text{ul}}, \quad \text{for all } k \text{ and } j \quad (16)$$

where the auxiliary variables are $z^{\text{dl}} = [z_{kj}^{\text{dl}}]_{k=1, j=1}^{k=K, j=J}$ and $z^{\text{ul}} = [z_{kj}^{\text{ul}}]_{k=1, j=1}^{k=K, j=J}$. However, the above substitution is difficult to implement; thus, we use standard big- M [9] to enforce the above equality. The constraints are as follows:

$$0 \leq z_{kj}^{\text{dl}} \leq t_k^{\text{dl}}, 0 \leq z_{kj}^{\text{ul}} \leq t_k^{\text{ul}}, \quad (17a)$$

$$t_k^{\text{dl}} - M(1 - d_{kj}) \leq z_{kj}^{\text{dl}} \leq Md_{kj}, \quad (17b)$$

$$t_k^{\text{ul}} - M(1 - u_{kj}) \leq z_{kj}^{\text{ul}} \leq Mu_{kj}. \quad (17c)$$

Note, applying big- M , we don't lose any optimality as the above constraints, enforces the equality in (16) exactly if the value of M chosen properly [9]. Finally, the problem in (P3) is written with big- M constraints as

$$\begin{aligned} \text{(P4)} : \quad & \max_{\mathbf{d}, \mathbf{u}, \mathbf{t}^{\text{dl}}, \mathbf{t}^{\text{ul}}, \mathbf{z}^{\text{dl}}, \mathbf{z}^{\text{ul}}, \boldsymbol{\chi}^{\text{dl}*}, \boldsymbol{\chi}^{\text{ul}*}, \boldsymbol{\xi}^{\text{dl}*}, \boldsymbol{\xi}^{\text{ul}*}} f_3(\mathbf{d}, \mathbf{r}, \mathbf{u}, \mathbf{t}^{\text{dl}}, \mathbf{t}^{\text{ul}}, \mathbf{z}^{\text{dl}}, \mathbf{z}^{\text{ul}}, \boldsymbol{\chi}^{\text{dl}*}, \boldsymbol{\chi}^{\text{ul}*}, \boldsymbol{\xi}^{\text{dl}*}, \boldsymbol{\xi}^{\text{ul}*}), \\ \text{s.t.} \quad & \left| \sum_{j \in \mathcal{J}} d_{kj} r_j - \sum_{j \in \mathcal{J}} u_{kj} r_j \right| \\ & \leq M(2 - \sum_{j \in \mathcal{J}} d_{kj} - \sum_{j \in \mathcal{J}} u_{kj}), \forall k \quad (19a) \\ & \sum_{k \in \mathcal{K}} (z_{kj}^{\text{dl}})^2 \leq p_j^{\text{max}}, \text{ for all } j \quad (19b) \\ & \text{(8b), (8d) - (8f), (17a) - (17c).} \quad (19c) \end{aligned}$$

where in (19a), we enforce the same logic in (8a) by a large number M for ease of implementation in solvers. The objective f_3 is shown at the bottom in (18), which is concave in z_{kj}^{dl} and z_{kj}^{ul} . Further, continuous relaxation of feasible set is convex. Therefore, the program can be solved to optimality with standard techniques, e.g., branch & bound, and convex optimization, implemented in industry grade solvers, e.g., MOSEK, which is used here.

As mentioned before, the value of M must be chosen properly. First, in constraint (17), a suitable value is $M \geq \max_{k,j} \{\sqrt{p_j^{\text{max}}}, \sqrt{p_k^{\text{max}}}\}$ [9]. Additionally, we also used M for conditional switch in (19a), for this M must be $\geq \max_k |\sum_{j \in \mathcal{J}} d_{kj} r_j - \sum_{j \in \mathcal{J}} u_{kj} r_j|$; whose maximum value is 1, due to constraint (8b). Combining two conditions, we choose, $M = \lceil \max\{\max_{k,j} \{\sqrt{p_j^{\text{max}}}, \sqrt{p_k^{\text{max}}}\}, 1\} \rceil$, where $\lceil \cdot \rceil$ denotes the smallest integer function.

Algorithm 1 Solution for optimization (P0)

```

1: for all  $\mathbf{r} = [r_1, \dots, r_J] \in \{0, 1\}^J$  do
2:   Initialize: feasible values of  $\mathbf{d}, \mathbf{u}, \mathbf{p}^{\text{dl}}, \mathbf{p}^{\text{ul}}$ 
3:   repeat
4:     update  $\boldsymbol{\chi}^{\text{dl}}, \boldsymbol{\chi}^{\text{ul}}$  by (13)
5:     update  $\boldsymbol{\xi}^{\text{dl}}, \boldsymbol{\xi}^{\text{ul}}$  by (14)
6:     solve (P4) to get  $\mathbf{d}, \mathbf{u}, \mathbf{p}^{\text{dl}}, \mathbf{p}^{\text{ul}}$ 
7:   until convergence
8: end for
9: select  $(\mathbf{d}^\dagger, \mathbf{r}^\dagger, \mathbf{u}^\dagger, \mathbf{p}^{\text{dl}\dagger}, \mathbf{p}^{\text{ul}\dagger}, \boldsymbol{\chi}^{\text{dl}\dagger}, \boldsymbol{\chi}^{\text{ul}\dagger}, \boldsymbol{\xi}^{\text{dl}\dagger}, \boldsymbol{\xi}^{\text{ul}\dagger})$  corresponding to the highest achieved objective value  $f_2$  over all feasible  $\mathbf{r}$ . Then, the optimal objective  $f_0$  is obtained from (7) using  $(\mathbf{d}^\dagger, \mathbf{r}^\dagger, \mathbf{u}^\dagger, \mathbf{p}^{\text{dl}\dagger}, \mathbf{p}^{\text{ul}\dagger})$ .

```

Finally, the complete solution procedure is outlined in Algorithm 1. The algorithm iterates over all binary combinations of \mathbf{r} . For each fixed \mathbf{r} , the variables $\mathbf{d}, \mathbf{u}, \mathbf{p}^{\text{dl}}, \mathbf{p}^{\text{ul}}$ are initialized to satisfy (8a)–(8f). Then, the variables are updated block-wise: step-4: update $\boldsymbol{\chi}^{\text{dl}}, \boldsymbol{\chi}^{\text{ul}}$ by (13); step-5: update $\boldsymbol{\xi}^{\text{dl}}, \boldsymbol{\xi}^{\text{ul}}$ by (14); and step-6: solve (P4) to obtain $\mathbf{d}, \mathbf{u}, \mathbf{p}^{\text{dl}}, \mathbf{p}^{\text{ul}}$. These updates repeat until convergence for each \mathbf{r} , after convergence, select $(\mathbf{d}^\dagger, \mathbf{r}^\dagger, \mathbf{u}^\dagger, \mathbf{p}^{\text{dl}\dagger}, \mathbf{p}^{\text{ul}\dagger}, \boldsymbol{\chi}^{\text{dl}\dagger}, \boldsymbol{\chi}^{\text{ul}\dagger}, \boldsymbol{\xi}^{\text{dl}\dagger}, \boldsymbol{\xi}^{\text{ul}\dagger})$ corresponding to the highest achieved objective value f_2 . Then, the optimal f_0 is obtained from (7).

Proposition 2. *Algorithm 1 converges in a finite number of iterations. Further, it has at least one limit point, and every limit point is a stationary point for $\boldsymbol{\chi}^{\text{dl}}, \boldsymbol{\chi}^{\text{ul}}, \boldsymbol{\xi}^{\text{dl}},$ and $\boldsymbol{\xi}^{\text{ul}}$.*

Proof. See Appendix B. □

IV. NUMERICAL RESULTS

In this section, we present the numerical results corresponding to the above formulations. We consider a scenario where $K = 10$ randomly distributed UEs are placed within a circular region of radius 100 m centered around location (53.0793°N, 8.8017°E). These UEs are served by J satellites. The frequency bands are $f_1 = 2.4$ GHz and $f_2 = 1.9$ GHz, with $B_1 = B_2 = 10$ MHz. Each satellite is equipped with $N = 16 \times 16$ antennas arranged in a uniform-planar array (UPA) configuration. The inter-UE channels are modeled as purely LOS. The maximum transmit power at each satellite is 20 W, while the UEs transmit with a maximum power of 2 W in the UL direction. The satellites are positioned at an

$$\begin{aligned} f_3(\mathbf{d}, \mathbf{r}, \mathbf{u}, \mathbf{t}^{\text{dl}}, \mathbf{t}^{\text{ul}}, \mathbf{z}^{\text{dl}}, \mathbf{z}^{\text{ul}}, \boldsymbol{\chi}^{\text{dl}}, \boldsymbol{\chi}^{\text{ul}}, \boldsymbol{\xi}^{\text{dl}}, \boldsymbol{\xi}^{\text{ul}}) = & \sum_{k \in \mathcal{K}} \sum_{j \in \mathcal{J}} \left[\log_2(1 + \chi_{kj}^{\text{dl}}) + \log_2(1 + \chi_{kj}^{\text{ul}}) - \chi_{kj}^{\text{dl}} - \chi_{kj}^{\text{ul}} - (\xi_{kj}^{\text{dl}} \sigma)^2 - (\xi_{kj}^{\text{ul}} \sigma)^2 \right. \\ & + 2\xi_{kj}^{\text{dl}} z_{kj}^{\text{dl}} \sqrt{(1 + \chi_{kj}^{\text{dl}})} \|\boldsymbol{\gamma}_{kjj}^{\text{dl}}\| + 2\xi_{kj}^{\text{ul}} z_{kj}^{\text{ul}} \sqrt{(1 + \chi_{kj}^{\text{ul}})} \|\boldsymbol{\gamma}_{kjj}^{\text{ul}}\| - (z_{kj}^{\text{dl}})^2 \sum_{j' \in \mathcal{J}} \sum_{k' \in \mathcal{K}} (\xi_{k'j'}^{\text{dl}})^2 |(\boldsymbol{\gamma}_{k'j'j}^{\text{dl}})^T \mathbf{w}_{kj}|^2 \\ & \left. - (z_{kj}^{\text{ul}})^2 \sum_{j' \in \mathcal{J}-j} \sum_{k' \in \mathcal{K}-k} (\xi_{k'j'}^{\text{ul}})^2 |\nu_{k'k'j'j}|^2 - (z_{kj}^{\text{ul}})^2 \sum_{j' \in \mathcal{J}} \sum_{k' \in \mathcal{K}} (\xi_{k'j'}^{\text{ul}})^2 |\mathbf{v}_{k'j'}^T \boldsymbol{\gamma}_{k'j'j}^{\text{ul}}|^2 \right]. \quad (18) \end{aligned}$$

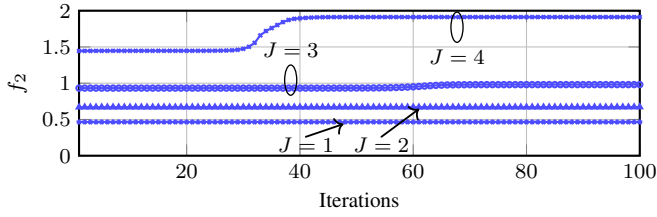


Fig. 4. Monotonic increase of f_2 with iterations for the proposed Algorithm 1.

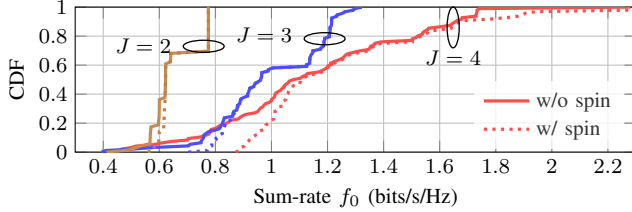


Fig. 5. CDF of the sum-rate f_0 with and without spin.

altitude of 500 km, each deployed at different elevation and inclination angles.

Figure 4 illustrates the evolution of the objective f_2 with iterations for $J = [2, 3, 4]$. It can be observed that the proposed algorithm converges within a finite number of steps, consistent with the convergence result established in Proposition 2.

Figure 5 shows the cumulative distribution function (CDF) of the sum-rate for $J = [2, 3, 4]$. In the proposed setup, the “with spin” configuration implies that each satellite j adaptively selects its r_j through the optimization. Conversely, in the “without spin” case, we fix $r_j = 0$ for all satellites j , which corresponds to a conventional non-adaptive configuration. It can be observed that for $J = 2$, both configurations exhibit nearly identical performance. This behavior arises from the strong inter-UE interference that occurs when the UEs operate in opposite spin states. Since the inter-UE channels are modeled as purely LOS, the benefits of frequency spin are effectively neutralized in this case. However, as the number of satellites increases, the interference level also grows, and the proposed “with spin” strategy demonstrates significant gains, approximately 78 % improvement for $J = 3$ and nearly 94 % improvement for $J = 4$ in the tail of the distribution, as illustrated in the figure.

V. CONCLUSIONS

This paper presented a dynamic band allocation framework for LEO satellite systems in 6G networks. By enabling satellites and users to jointly select DL and UL frequency bands, the approach adds flexibility to conventional FDD systems and enhances spectrum utilization. A joint optimization problem was formulated for dynamic band selection, user scheduling, and power allocation, and solved through efficient transformation-based methods. Simulation results showed that the proposed strategy effectively mitigates interference in dense constellations, achieving up to 94% performance improvement in high-interference scenarios.

APPENDIX

A. Proof of Proposition 1

Observe that f_2 is strictly concave in ξ^{dl} and in ξ^{ul} . Therefore, keeping other variables fixed, unique optimal point $\xi_{kj}^{\text{dl}*}$ and $\xi_{kj}^{\text{ul}*}$ is obtained from $\partial f_2 / \partial \xi_{kj}^{\text{dl}} = 0$ and $\partial f_2 / \partial \xi_{kj}^{\text{ul}} = 0$. Substituting this in f_2 recovers f_1 exactly. Similarly, f_1 is strictly concave in χ^{dl} and χ^{ul} . Therefore, unique optimal $\chi_{kj}^{\text{dl}*}$ and $\chi_{kj}^{\text{ul}*}$ can be obtained from $\partial f_1 / \partial \chi_{kj}^{\text{dl}} = 0$ and $\partial f_1 / \partial \chi_{kj}^{\text{ul}} = 0$. Substituting this in f_1 gives f_0 exactly. \square

B. Proof of Proposition 2

We introduce a subscript t for the iteration index, and we ignore the variable \mathbf{r} , as we search over all possible values. Therefore, for the objective f_2 the following holds:

$$\begin{aligned}
 & f_2(\mathbf{d}_{(t)}, \mathbf{u}_{(t)}, \mathbf{p}_{(t)}^{\text{dl}}, \mathbf{p}_{(t)}^{\text{ul}}, \boldsymbol{\chi}_{(t)}^{\text{dl}}, \boldsymbol{\chi}_{(t)}^{\text{ul}}, \boldsymbol{\xi}_{(t)}^{\text{dl}}, \boldsymbol{\xi}_{(t)}^{\text{ul}}) \\
 & \stackrel{(a)}{=} f_1(\mathbf{d}_{(t)}, \mathbf{u}_{(t)}, \mathbf{p}_{(t)}^{\text{dl}}, \mathbf{p}_{(t)}^{\text{ul}}, \boldsymbol{\chi}_{(t)}^{\text{dl}}, \boldsymbol{\chi}_{(t)}^{\text{ul}}) \\
 & \stackrel{(b)}{<} f_1(\mathbf{d}_{(t)}, \mathbf{u}_{(t)}, \mathbf{p}_{(t)}^{\text{dl}}, \mathbf{p}_{(t)}^{\text{ul}}, \boldsymbol{\chi}_{(t+1)}^{\text{dl}}, \boldsymbol{\chi}_{(t+1)}^{\text{ul}}) \\
 & \stackrel{(c)}{=} f_2(\mathbf{d}_{(t)}, \mathbf{u}_{(t)}, \mathbf{p}_{(t)}^{\text{dl}}, \mathbf{p}_{(t)}^{\text{ul}}, \boldsymbol{\chi}_{(t+1)}^{\text{dl}}, \boldsymbol{\chi}_{(t+1)}^{\text{ul}}, \boldsymbol{\xi}_{(t+1)}^{\text{dl}}, \boldsymbol{\xi}_{(t+1)}^{\text{ul}}) \\
 & \stackrel{(e)}{\leq} f_2(\mathbf{d}_{(t+1)}, \mathbf{u}_{(t+1)}, \mathbf{p}_{(t+1)}^{\text{dl}}, \mathbf{p}_{(t+1)}^{\text{ul}}, \boldsymbol{\chi}_{(t+1)}^{\text{dl}}, \boldsymbol{\chi}_{(t+1)}^{\text{ul}}, \boldsymbol{\xi}_{(t+1)}^{\text{dl}}, \\
 & \quad \boldsymbol{\xi}_{(t+1)}^{\text{ul}})
 \end{aligned}$$

where (a) follows from proof of Proposition 1, as keeping other variables fixed, f_2 is strictly concave in ξ^{dl} and ξ^{ul} . Therefore, we can obtain ξ^{dl} and ξ^{ul} uniquely as in (14) and substituting these in f_2 we get f_1 exactly. Further, (b) follows as f_1 is strictly concave in χ^{dl} and χ^{ul} ; therefore, until a stationary point is obtained, the objective strictly increases with each update. Then, (c) follows similar logic as in (a). Finally, (e) follows, as keeping other variables fixed, joint update of $(\mathbf{d}, \mathbf{u}, \mathbf{p}^{\text{dl}}, \mathbf{p}^{\text{ul}})$ maximizes the objective. Also, as the transmit powers are fixed, and the each update strictly increases the objective, the algorithm converges in finite steps. \square

REFERENCES

- [1] E. Yaacoub and M.-S. Alouini, “A key 6G challenge and opportunity—connecting the base of the pyramid: A survey on rural connectivity,” *Proc. IEEE*, 2020.
- [2] C. Braun, A. M. Voicu, L. Simic, and P. Mahonen, “Should we worry about interference in emerging dense NGSO satellite constellations?,” in *Proc. IEEE Int. Symp. Dyn. Spectr. Access Netw. (DySPAN)*, 2019.
- [3] M. Jalali, E. Lagunas, A. Haqiqatnejad, S. Kisseleff, and S. Chatzinotas, “Downlink beamforming strategies for interference-aware NGSO satellite systems,” *IEEE Open J. Commun. Soc.*, 2024.
- [4] H.-W. Lee, C.-C. Chen, C.-I. S. Liao, A. Medles, D. Lin, I.-K. Fu, and H.-Y. Wei, “Interference mitigation for reverse spectrum sharing in B5G/6G satellite-terrestrial networks,” *IEEE Trans. Veh. Technol.*, 2024.
- [5] H. Al-Hraishawi, H. Chougrani, S. Kisseleff, E. Lagunas, and S. Chatzinotas, “A survey on nongeostationary satellite systems: The communication perspective,” *IEEE Commun. Surv. & Tutorials*, 2023.
- [6] M. Takahashi, Y. Kawamoto, N. Kato, A. Miura, and M. Toyoshima, “Adaptive power resource allocation with multi-beam directivity control in high-throughput satellite communication systems,” *IEEE Wirel. Commun. Lett.*, 2019.

- [7] P. Popovski, O. Simeone, J. J. Nielsen, and Č. Stefanović, "Interference spins: Scheduling of multiple interfering two-way wireless links," *IEEE Commun. Lett.*, 2015.
- [8] K. Shen and W. Yu, "Fractional programming for communication systems—part II: Uplink scheduling via matching," *IEEE Trans. Signal Process.*, 2018.
- [9] A. DeJans Jr., *The Linearization Handbook for MILP Optimization: Modeling Tricks and Patterns for Practitioners*. BitBros Publisher, 2025.